

Proceedings of the  
International Conference on  
**HIGH SPIN PHYSICS and  
GAMMA-SOFT NUCLEI**

Pittsburgh, PA USA      September 17 – 21, 1990

Editors: J.X. Saladin

R.A. Sorensen

C.M. Vincent

University of Pittsburgh  
Carnegie Mellon University

# ALIGNMENT AND CORE POLARIZATION IN $f - p - g$ SHELL NUCLEI

S.L. TABOR<sup>a)</sup>, S.G. BUCCINO<sup>b)</sup>, P.D. COTTLE<sup>a)</sup>,  
F.E. DURHAM<sup>b)</sup>, C.J. GROSS<sup>a)</sup>, J.W. HOLCOMBE<sup>a)</sup>,  
U.J. HÜTTMEIER<sup>a)</sup>, T.D. JOHNSON<sup>a)</sup>,  
M. MATSUZAKI<sup>c)</sup>, E.F. MOORE<sup>a)</sup>,  
W. NAZAREWICZ<sup>d)</sup> AND P.C. WOMBLE<sup>a)</sup>

<sup>a)</sup>Physics Department, Florida State University  
Tallahassee, FL 32306 USA

<sup>b)</sup>Department of Physics, Tulane University  
New Orleans, LA 70118 USA

<sup>c)</sup>Institute of Physics, University of Tsukuba

Ibaraki 305, JAPAN

<sup>d)</sup>Institute of Physics

Warsaw Institute of Technology  
PL-00662 Warsaw, POLAND

## ABSTRACT

Although some  $f - p - g$  shell nuclei are highly deformed even at low spins ( $\beta_2 > 0.4$ ), the  $E_{4+}/E_{2+}$  ratios never exceed 2.9, falling significantly short of the rigid rotor value of 3.33. The behavior of the kinematic moments of inertia as a function of spin and nucleon number is examined to better understand the energy ratios. The behavior is also seen to depend on the number of unpaired particles. Experimental and theoretical evidence suggests that two moderately deformed shapes coexist in  $^{74}\text{Kr}$  and  $^{74}\text{Se}$ , one prolate and one oblate. Several different shapes coexist in  $^{81}\text{Sr}$  depending on which Nilsson orbital is occupied. The magnitude of signature splitting varies considerably among these nuclei and can lead to alternating magnetic transition strengths and phase reversals.

## 1. OVERVIEW

Nuclei in the  $f - p - g$  shell are the heaviest in which neutrons and protons fill the same unique parity orbital ( $g_{9/2}$ ). They are particularly soft or sensitive

to polarizing influences. Quadrupole deformations  $\beta_2$  in excess of 0.4 have been observed, yet highly deformed shapes often "coexist" with nearly spherical ones.

### 1.1 Systematics of Energy Ratios and Deformations

One significant difference between  $f - p - g$  shell nuclei and their heavier counterparts can be seen in the ratios of the energies of the lowest  $4^+$  to  $2^+$  states in Fig. 1. While most of the  $E_{4^+}/E_{2^+}$  ratios lie above the value of 2.0 expected for an ideal vibrator, they do not approach very closely to the value of 3.33 expected for an ideal rotor. The highest values reached are only 2.86 ( $^{80}\text{Zr}$ , Ref. 1) and 2.90 ( $^{78}\text{Sr}$ , Ref. 2).

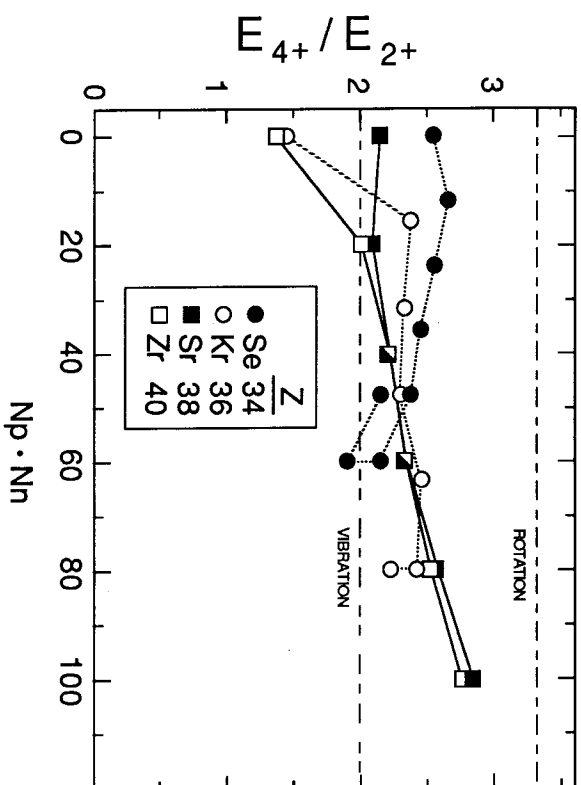


Fig. 1. Ratios of the lowest  $4^+$  to  $2^+$  energies in even-even nuclei as a function of  $N_p N_n$ .  $N_p(N_n)$  is the number of proton (neutron) particles or holes in the 28 - 50 shell.

The usual interpretation of such evidence, that these nuclei are not very deformed or collective, is contradicted by the strong electromagnetic transitions. For example, the quadrupole deformations  $\beta_2$  calculated from the  $B(E2, 2^+ \rightarrow 0^+)$  transition strengths assuming an axially symmetric rotational model are shown in Fig. 2. Most show well deformed values above 0.2, five exceed 0.3 and one reaches the highly deformed value of 0.45. The list of high  $\beta_2$  values would be longer if

lifetimes were known for the lighter Sr and Kr isotopes. Many of the odd A and odd-odd nuclei are also highly deformed.

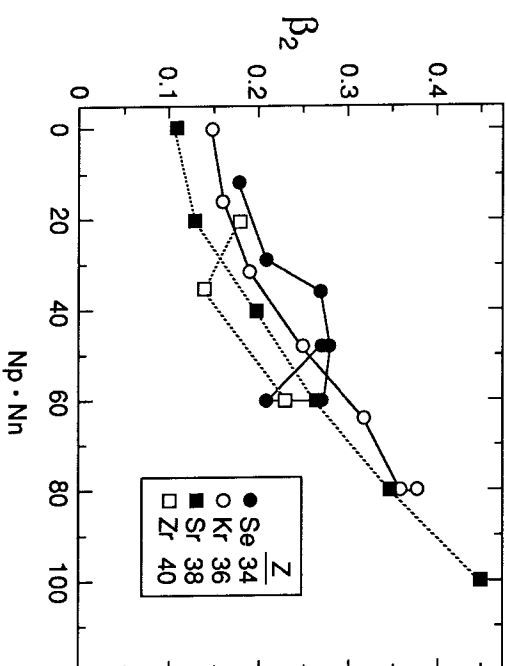


Fig. 2. Quadrupole deformations  $\beta_2$  inferred from  $B(E2: 2^+ \rightarrow 0^+)$  assuming a rotor model and axial symmetry.

Hence the low-spin energy ratios reflect nuclear deformation in  $A \approx 80$  nuclei more poorly than in heavier nuclei. A number of factors may contribute to this effect, including shape coexistence and gradual alignments. The discussion of Sec. 1.2 is also relevant to this question.

The abscissa in these graphs is proportional to the number of deformation driving  $n-p$  pairs. It was shown earlier<sup>3)</sup> that energy differences not involving the ground states vary much more systematically with  $N_p N_n$  than does  $E_{4^+}/E_{2^+}$ . The deformations in Fig. 2 increase more regularly with  $N_p N_n$  except for the Se isotopes.

### 1.2 Systematics of the Moments of Inertia

A further examination of deformation and alignment trends in  $f - p - g$  shell nuclei is provided by calculating their kinematic moments of inertia  $J^{(1)}$  from the measured level spacings. Some of the trends are seen most clearly in the even Sr isotopes shown in Fig. 3a. The moment of inertia starts rather low in even

the most deformed isotope  $^{78}\text{Sr}$  ( $\beta_2 \approx 0.45$ ) and increases steadily with increasing rotational frequency. The total change is a factor of 2 over the measured range.

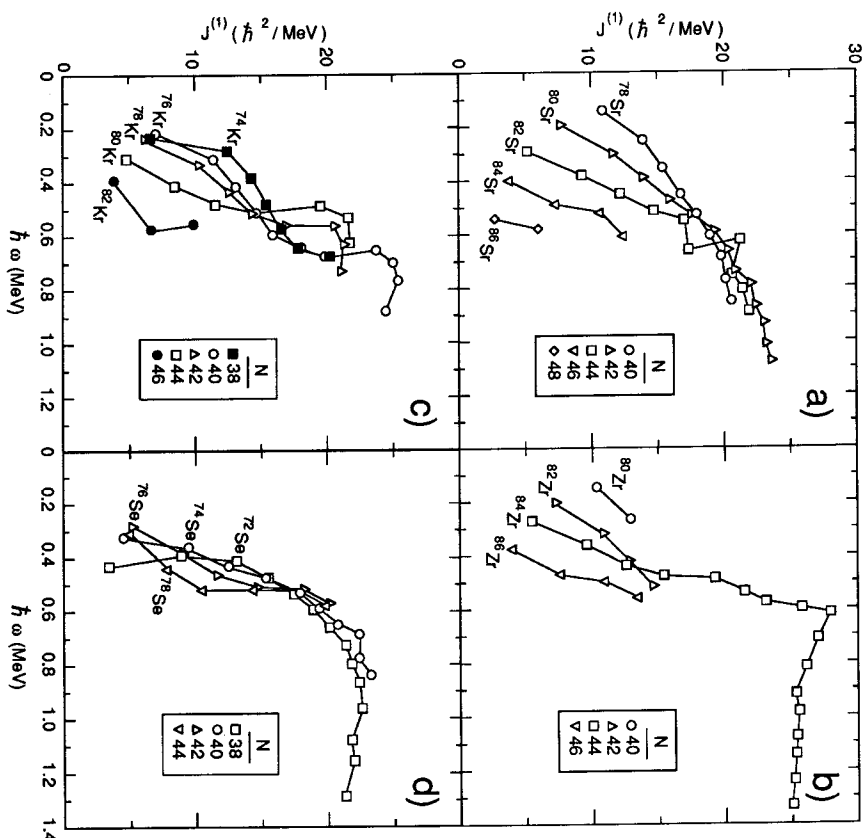


Fig. 3. The kinematic moments of inertia  $J^{(1)}$  as a function of rotational frequency  $\omega$  for the Se ( $Z=34$ ), Kr ( $Z=36$ ), Sr ( $Z=38$ ) and Zr ( $Z=40$ ) isotopes.

The moments of inertia for the lowest spin states decrease steadily as the neutron number increases from mid-shell ( $N=38-40$ ) towards the shell closure at  $N=50$ . This is the same trend seen in Fig. 2 because  $N_p \cdot N_n$  decreases as  $N$  increases, since  $N_n$  is counted as the number of neutron holes above mid-shell. Another interesting and somewhat compensating trend is also apparent in Fig. 3. As the initial  $J^{(1)}$  values decrease, their rate of increase with frequency grows steeper. The net result is a tendency for the  $J^{(1)}$  values to converge above  $\hbar\omega \approx 0.6$

MeV towards a common curve, which itself approaches saturation at about  $24 \hbar^2/\text{MeV}$ , approximately the rigid body value. Espino and Garrett<sup>4</sup>) have shown that rare earth nuclei also tend to converge to a common moment of inertia at high spins.

Of course, these are only trends. Sharp alignments occur along the way, as in the case of  $^{82}\text{Sr}$ , and the ground state bands (GSB) of the heavier nuclei are not known to higher spins. Less is known about the even Zr isotopes, except for  $^{84}\text{Zr}$ . Nevertheless, the features discussed above can be seen in Fig. 3b. Some of the systematics are less clear in the lighter elements, Kr (Fig. 3c) and Se (Fig. 3d), although the general rise in  $J^{(1)}$  with  $\omega$  is always present. One complication is that the lowest  $^{74}\text{Kr}$  point lies significantly below an expected position extrapolated from the higher frequency points. This effect, which has been interpreted as arising from shape coexistence<sup>5,6</sup>) is also present to a lesser extent in  $^{76,78}\text{Kr}$ . The  $J^{(1)}$  values for the second and third frequency points decrease with increasing  $N$ , while their slopes increase. Shape coexistence has an even more dramatic effect on the Se isotopes, so that only the third frequency points follow the ordering of the heavier elements. A saturation of  $J^{(1)}$  at about  $22 \hbar^2/\text{MeV}$  can be seen for  $^{72}\text{Se}$ .

The rapid change in  $J^{(1)}$  in Fig. 3 for the low spins leads to the reduced  $E_4+/E_{2+}$  ratios in Fig. 1. The systematic variation of  $J^{(1)}$  with  $N$  for the Sr and Zr isotopes is related to the systematic variation of  $E_4+/E_{2+}$  with  $N_p \cdot N_n$ , while its lack of variation with  $N$  for the Se and Kr isotopes corresponds to the more constant behavior of  $E_4+/E_{2+}$ .

## 2. ODD PARTICLES AND THE MOMENT OF INERTIA

The increasing trends in the kinematic moments of inertia  $J^{(1)}$  discussed in Sec. 1.2 are characteristic of the yrast bands in even-even nuclei in the  $f-p-g$  shell. Figure 4 illustrates some of the effects of odd particles on  $J^{(1)}$ . Again the moments of inertia start from very different values and converge to a common value at high rotational frequencies. The difference is that  $J^{(1)}$  remains rather constant for the yrast band in odd Z  $^{73}\text{Br}$ , rather than increasing, and actually decreases to convergence in odd-odd  $^{74,76}\text{Br}$ . There are indications from the behavior of the signature splitting in  $^{74,76}\text{Br}$  (see Sec. 4.2) that increasing alignment of the two odd particles plays a key role in the low spin region.

Even in an even-even nucleus  $J^{(1)}$  for excited bands may behave very differently. For example, the graph of  $J^{(1)}$  for the  $K^\pi=3^-$  band in  $^{74}\text{Se}$  resembles that of  $^{73}\text{Br}$  in Fig. 4, even though the transition quadrupole moments are very similar<sup>7</sup>) to those of the GSB.

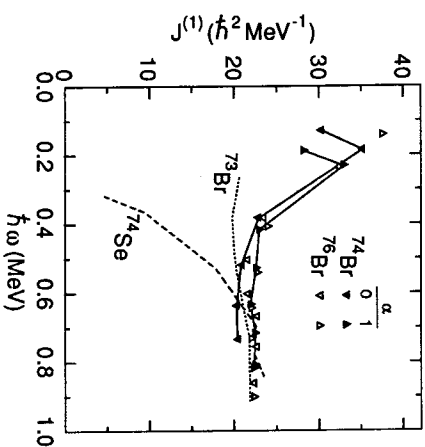


Fig. 4. A comparison of kinematic moments of inertia for even, odd and odd-odd nuclei.

### 3. SHAPE COEXISTENCE

#### 3.1 $^{74}\text{Kr}$ and $^{74}\text{Se}$

The interpretation of the low spin anomalies in  $J^{(1)}$  as arising from shape coexistence was discussed in Sec. 1.2. The anomalously low first points for  $^{74}\text{Kr}$  and  $^{74}\text{Se}$  in Fig. 3 arise from distortions in the energy level spacings, especially the overly large  $2^+-0^+$  energy difference. Two level mixing calculations involving a well deformed band and a weakly deformed band have accounted<sup>(6,8)</sup> reasonably well for the distortions in the GSB energies.

However, a recent experimental investigation<sup>(7)</sup> of  $^{74}\text{Se}$  and Hartree-Fock-Bogolyubov (HFB) cranking calculations<sup>(5,7)</sup> for  $^{74}\text{Kr}$  and  $^{74}\text{Se}$  suggest that two well-deformed configurations coexist at low spins. The total Routhian surfaces (TRS) in Fig. 5 calculated for  $^{74}\text{Kr}$  show two energy minima. The graph for  $\hbar\omega \approx 0.40$  MeV is typical of those below the first band crossing. The absolute minimum lies along the prolate axis at a relatively high deformation of  $\beta_2 \approx 0.37$ . A secondary oblate minimum with a slightly lower deformation of  $\beta_2 \approx 0.33$  can also be seen. The TRS for  $^{74}\text{Se}$  also show two energy minima, a well deformed, nearly prolate absolute minimum ( $\beta_2 \approx 0.32$ ,  $\gamma \approx 10^\circ$ ) and a secondary oblate minimum which is somewhat less deformed ( $\beta_2 \approx 0.23$ ).

The experimental observation of strong E2 transitions connecting a second band with the GSB of  $^{74}\text{Se}$  and the reassessment of a spin assignment have led to the interpretation<sup>(7)</sup> of the second band as another  $K^\pi=0^+$  band. The kinematic

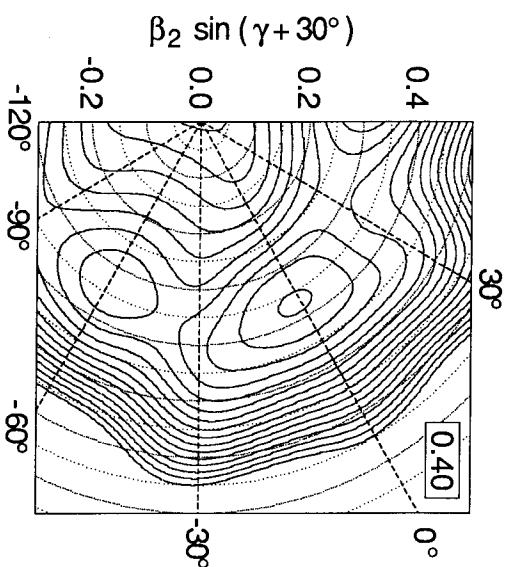


Fig. 5. Theoretical total Routhian surfaces in the  $(\beta_2, \gamma)$  plane for  $^{74}\text{Kr}$  at  $\hbar\omega = 0.40$  MeV. The contour spacing is 500 keV.

moments of inertia for the two bands are shown in Fig. 6. Lifetime measurements in the GSB indicate axial deformations  $\beta_2$  ranging from 0.26 to 0.36. Although lifetimes are not known in the  $0_2^+$  band because of its weaker population, its deformation must be at least as large as that of the GSB, since its moment of inertia is larger than that of the GSB. Hence the experimental evidence also suggests that two moderately to well-deformed shapes coexist.

Some interesting alignments can also be seen in Fig. 6. A linear sequence of  $J^{(1)}$  points in what is labeled as one band appears to continue into the other band. This is shown by the dashed straight lines and possibly the dotted line. The two dashed lines intersect, indicating a crossing at  $\hbar\omega = 0.4$  MeV.

#### 3.2 $^{81}\text{Sr}$ and $^{83}\text{Zr}$

The nucleus  $^{81}\text{Sr}$  provides a good example<sup>(9-11)</sup> of another kind of shape coexistence where substantially different shapes are stabilized by a single particle. The level scheme in Fig. 7 shows 4 rotational bands built on different  $\nu$  quasi-particle configurations. Lifetime measurements in the yrast  $g_{9/2}$  band on the left indicate a moderate axial deformation of  $\beta_2 \approx 0.21$ . HFB cranking calculations predict a similar degree of deformation and a nearly oblate shape,  $\beta_2 = 0.23$ ,  $\gamma =$

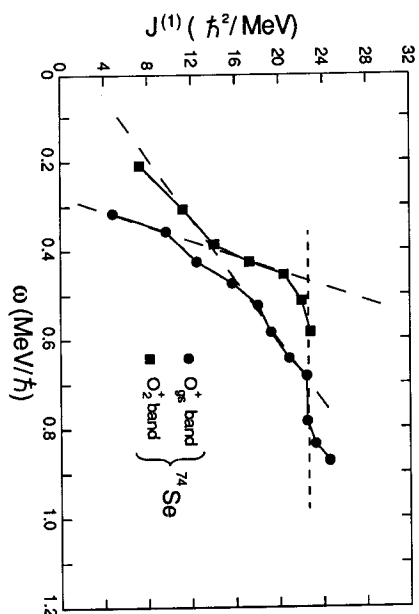


Fig. 6. Kinematic moments of inertia for two  $0^+$  bands in  $^{74}\text{Se}$ .

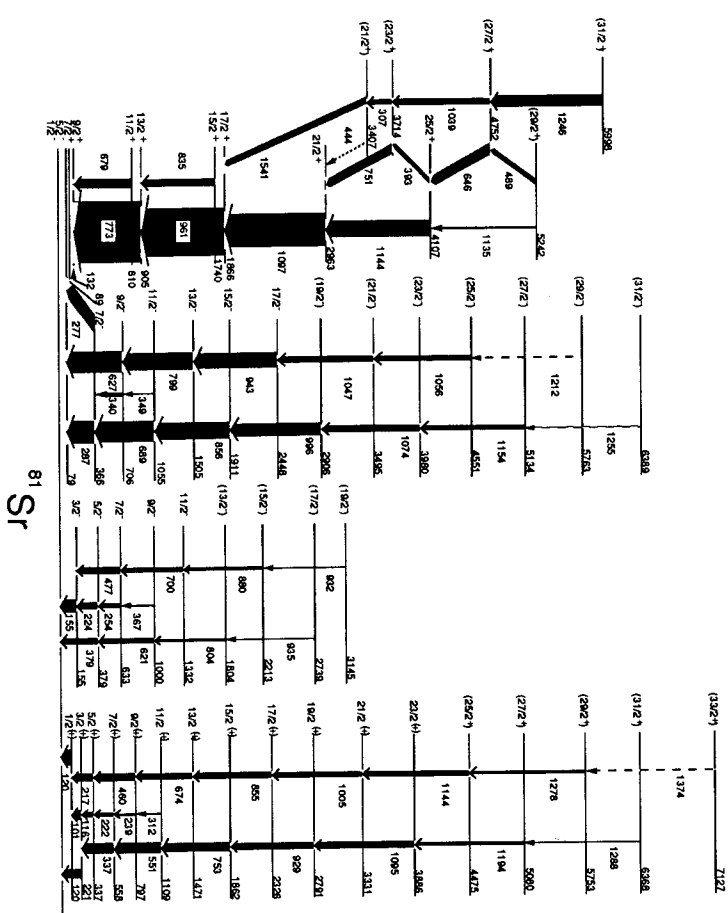


Fig. 7. The high spin energy level scheme of  $^{81}\text{Sr}$ .

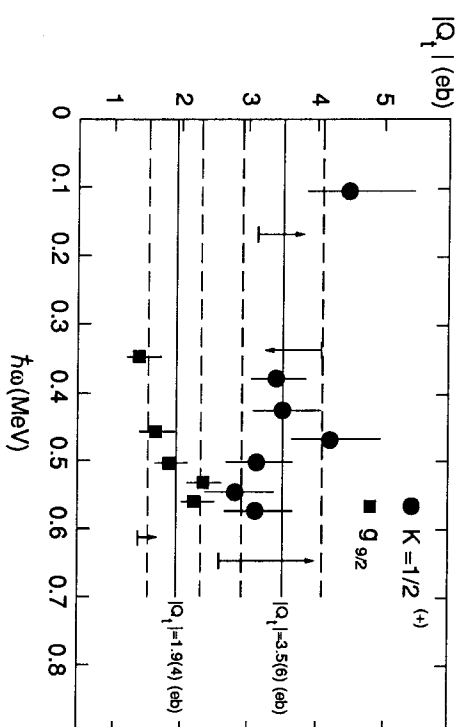


Fig. 8. The transition quadrupole moments inferred from the lifetimes for the yrast and  $1/2^+$  bands in  $^{81}\text{Sr}$ .

-  $50^\circ$ . A negative quadrupole moment and, hence, oblate shape was inferred<sup>(12)</sup> experimentally from mixing ratio measurements in a similar band in the isotope  $^{83}\text{Zr}$ . Lifetimes in the  $K^\pi=5/2^-$  band also imply a moderate deformation, and theoretically a near prolate shape is predicted for both this and the  $K^\pi=1/2^-$  bands.

The smaller energy spacings in the  $K^\pi=1/2^+$  band on the right imply a larger deformation. The transition quadrupole moments inferred from the lifetimes (Fig. 8) average about 3.5 eb, nearly twice as large as in the yrast  $g_{9/2}$  band, and confirm a high deformation  $\beta_2 \approx 0.4$ . Theoretically, the  $[431]1/2$  intruder orbital polarizes the core to a highly deformed prolate shape. So far as we know this intruder band has not been observed in neighboring nuclei, although it is predicted<sup>(11)</sup> to lie relatively low in several  $N=41$  and 43 isotones. An even more highly deformed intruder band which has been predicted, but not observed, would lie in  $^{83}\text{Zr}$ . The HFB cranking calculations for  $^{83}\text{Zr}$  predict<sup>(13)</sup> that an  $h_{11/2}$  prolate band with  $\beta_2 \approx 0.5$  would become yrast at  $\hbar\omega \approx 1.1$  MeV, a rotational frequency which has been reached only in  $^{84}\text{Zr}$ .

## 4. SIGNATURE SPLITTING AND MAGNETIC TRANSITIONS

The  $^{81}\text{Sr}$  level scheme in Fig. 7 illustrates some of the patterns of signature splitting and M1 decays seen in  $f-p-g$  shell nuclei. The large signature splitting in the  $g_{9/2}$  yrast band is rather typical of the odd  $A$  nuclei. In some nuclei, such as  $^{81}\text{Rb}$  (Ref. 14), the splitting is so large that the level ordering is inverted. There is very little signature splitting in the  $5/2^-$  band, as is typical, and, rather surprisingly, very little in the two  $K=1/2$  bands.

The reduction in signature splitting after the quasiparticle alignment in the yrast band has been seen in other nearby nuclei, such as  $^{79}\text{Kr}$  (Ref. 15) and  $^{81}\text{Kr}$  (Ref. 16). It appears to be caused by shape changes driven by the extra quasiparticles.

The magnetic transitions do not appear to be very strong, except in the 3 quasiparticle yrast band where the magnetic moments of the two rotation aligned quasiparticles add constructively with that of the deformation aligned quasineutron.

4.1  $^{77}\text{Kr}$ 

The  $^{77}\text{Kr}$  nucleus provides a good opportunity to study the relation between M1 transition strengths and signature splitting. The  $\Delta J=1$  transitions compete successfully with E2 decays up to spin  $33/2$  in the yrast band, higher than in neighboring nuclei. As can be seen in Fig. 9, the signature splitting rises significantly up to the band crossing, drops nearly to zero, and then rises again.

A Nilsson potential calculation assuming an axial prolate deformation of  $\beta_2=0.31$  in the 1 quasiparticle band and  $\beta_2=0.33$ ,  $\gamma=12^\circ$  after the crossing reproduces the behavior of the signature splitting and the general magnitude of the transition quadrupole moments.

An alternating pattern can be seen in the M1 strengths. The alternations are related to the signature splitting and are reproduced rather well by the same calculations. The increase after alignment may be related to the constructive addition of quasiparticle magnetic moments.

4.2  $^{74}\text{Br}$  and  $^{76}\text{Br}$ 

The  $K^\pi=4^+$  yrast bands of odd-odd  $^{74}\text{Br}$  and  $^{76}\text{Br}$  are very similar and provide another view on signature splitting and M1 strengths. The ordinate of the lower graph in Fig. 10 is related to the moment of inertia and would be a constant value of  $\hbar^2/2I$  for an ideal rotor. Signature splitting leads to an alternating pattern in the graph, as can be seen for  $^{75}\text{Kr}$ .

An alternating pattern can also be seen for the yrast bands of  $^{74}\text{Br}$  and  $^{76}\text{Br}$ . However, a careful examination reveals an unusual anomaly. The phase of the alternations, or signature splitting, abruptly reverses at a spin of 9 or  $11\hbar$ , as indicated by the arrows. Such a phase reversal is not seen for odd  $^{75}\text{Kr}$ .

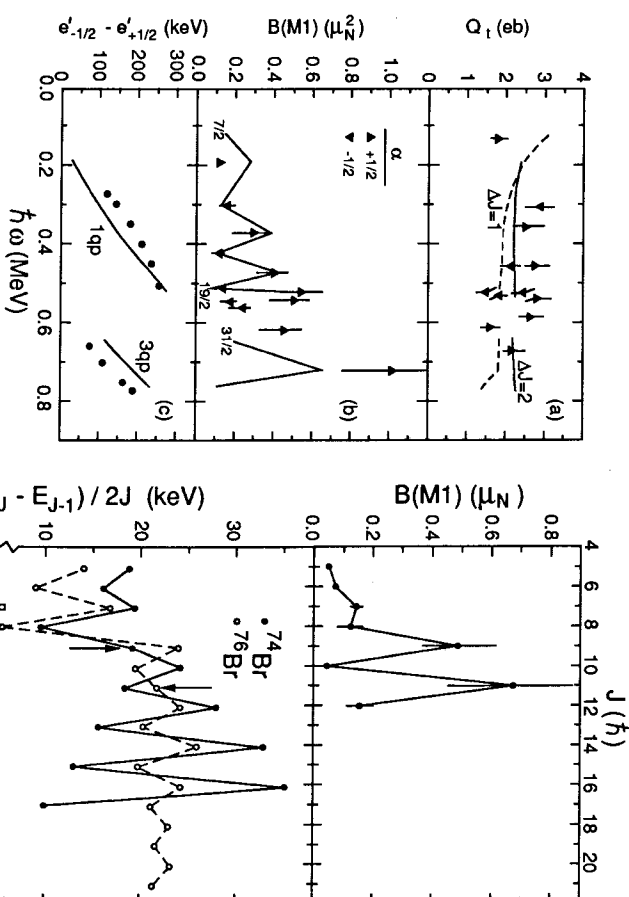


Fig. 9. A comparison of experimental and theoretical values for the transition quadrupole moments  $Q_t$ ,  $B(M1)$  strengths and signature splittings for  $^{77}\text{Kr}$ .

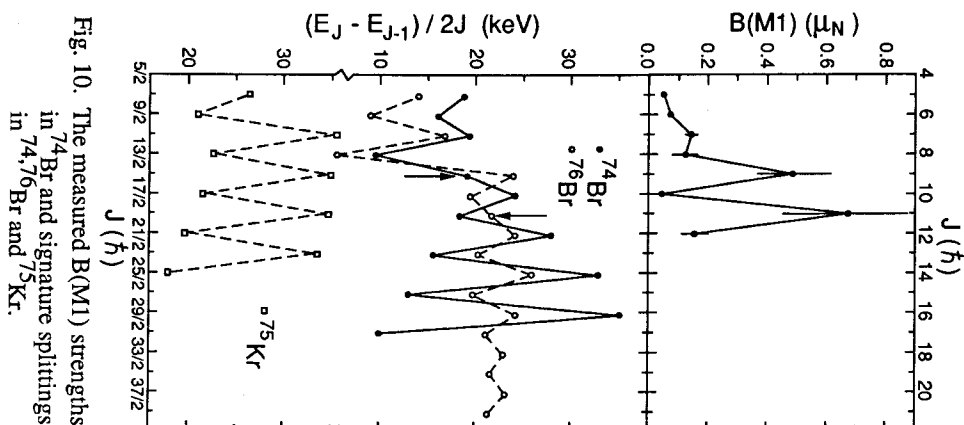


Fig. 10. The measured  $B(M1)$  strengths in  $^{74}\text{Br}$  and signature splittings in  $^{74,76}\text{Br}$  and  $^{75}\text{Kr}$ .

Kreiner and Mariscotti<sup>17)</sup> predicted such a reversal in the signature splitting in  $^{76}\text{Br}$  above  $9\hbar$  based upon calculations in a two interacting quasiparticles plus rotor model. The significance of spin 9 is that it represents the highest value obtainable from the intrinsic motion of two  $g_{9/2}$  particles in an odd-odd nucleus. Below it in the calculation, the yrast states are based on a combination of collective rotation

and realignment of the intrinsic spins. Above  $9\hbar$  the band involves rotation of a system with two fully aligned quasiparticles. Hamamoto<sup>18)</sup> has also shown that a similar reversal in signature splitting in  $^{156}\text{Tb}$  and  $^{160}\text{Ho}$  can be accounted for in a two quasiparticle plus rotor framework. The change also occurs near  $j_p + j_n$ .

The signature splitting also gives rise to an alternation in the M1 strengths, shown in the top part of Fig. 10. The pattern is consistent with the calculations of Hamamoto for  $^{156}\text{Tb}$  which show  $B(M1)$  strengths alternating out of phase with the energy differences.

## 5. SUMMARY

While the phenomena displayed by the deformed  $f - p - g$  shell nuclei may not be unique, the relative magnitudes of some effects are larger in this region, where fewer particles are involved and the shapes are so sensitive to various influences. For example, the number of nuclei attaining the rotational value for  $E_4 + E_2 +$  seems to decrease with mass, but none exceed 2.9 in the  $A \approx 80$  region. Perhaps there is a correlation with the number of active  $n - p$  pairs, but the limitation is not due to a lack of deformation or collectivity.

Some trends which emerge from the moments of inertia of the GSB in the even-even nuclei are considerable increases with frequency (by factors of 2 to 5) and a tendency to converge to a common value at higher frequencies. The tendency for  $J^{(1)}$  to converge above  $0.6 \text{ MeV}/\hbar$  extends to odd and odd-odd nuclei and excited bands. In many cases  $J^{(1)}$  remains relatively constant, and it even decreases with frequency for some odd-odd nuclei. The dependence of the  $J^{(1)}$  frequency trends on the number of quasiparticles and the relatively constant behavior of the transition quadrupole moments suggest that gradual quasiparticle alignment may play a key role in the  $J^{(1)}$  systematics.

The coexistence of significantly different nuclear shapes differing little in energy is not uncommon in  $f - p - g$  shell nuclei. The mixing of rotational bands based on two different shapes can account for such features as the perturbation of the energy levels which are particularly common in the lighter nuclei. HFB cranking calculations and lifetime measurements suggest that, at least in some cases, the coexisting shapes may both be moderately deformed and differ mainly in  $\gamma$ . In odd nuclei bands built on different Nilsson orbitals may differ substantially in shape.  $^{81}\text{Sr}$  provides a particularly good case where four bands have been followed up in spin. The corresponding shapes vary from moderately deformed oblate to moderately deformed prolate to highly deformed prolate.

Signature splitting is an observable quantity which provides information on

quasiparticle configurations, alignments and nuclear shapes. It also has a significant effect on magnetic transition strengths. The signature splittings in  $f - p - g$  shell nuclei vary from non-existent to inversions of the energy levels. In  $^{77}\text{Kr}$  the signature splitting varies considerably with rotational frequency and changes upon quasiparticle alignment. The magnetic transition strengths alternate depending on the signatures of the parent or daughter states. Those signature effects can be understood in a theoretical context. In  $^{74,76}\text{Br}$  the phase of the signature splitting actually reverses around spin 9, the maximum possible from two  $g_{9/2}$  particles. In the particle-rotor model this results from the importance of particle alignment at low spins and collective rotation at higher spins. The M1 strengths also alternate.

The  $f - p - g$  shell nuclei remain a fertile testing ground for many of the questions relating to the interplay between single particle and collective degrees of freedom. The effects of quasiparticles and quasiparticle alignment upon such collective phenomena as moments of inertia and nuclear shape and the effects of collective rotation on quasiparticle energies and pairing lie at the heart of the relation between the physics of the few and the many particles. The new generation of detector arrays offers many exciting possibilities for exploring this relationship.

## REFERENCES

- 1) C.J. Lister, M. Campbell, A.A. Chisti, W. Gellely, L. Goettig, R. Moscrop, B.J. Varley, A.N. James, T. Morrison, H.G. Price, J. Simpson, K. Connel and O. Skeppstedt, *Phys. Rev. Lett.* **59**, 1270 (1987).
- 2) C.J. Gross, J. Heese, K.P. Lieb, C.J. Lister, B.J. Varley, A.A. Chisti, J.H. McNeill and W. Gellely, *Phys. Rev. C* **39**, 1780 (1989).
- 3) S.L. Tabor, *Phys. Rev. C* **34**, 311 (1986).
- 4) J.M. Espino and J.D. Garrett, *Nucl. Phys. A* **492**, 205 (1989).
- 5) S.L. Tabor, P.D. Cottle, J.W. Holcomb, T.D. Johnson, P.C. Womble, S.G. Buccino and F.E. Durham, *Phys. Rev. C* **41**, 2658 (1990).
- 6) R.B. Piercey, J.H. Hamilton, R. Soundranayagam, A.V. Ramayya, C.F. Maguire, X.-J. Sun, Z.Z. Zhao, R.L. Robinson, H.J. Kim, S. Fraundorf, J. Döring, L. Funke, G. Winter, J. Roth, L. Cleeman, J. Eberth, W. Neumann, J.C. Wells, J. Lin, A.C. Rester, and H.K. Carter, *Phys. Rev. Lett.* **47**, 1514 (1981).
- 7) P.D. Cottle, J.W. Holcomb, T.D. Johnson, K.A. Snuckey, S.L. Tabor, P.C. Womble, S.G. Buccino and F.E. Durham, *Phys. Rev. C* (in press).
- 8) R.B. Piercey, A.V. Ramayya, R.M. Ronningen, J.H. Hamilton, V. Maruhn-Rezwani, R.L. Robinson and H.J. Kim, *Phys. Rev. C* **19**, 1344 (1979).
- 9) S.E. Arnell, C. Ekström, L.P. Ekström, A. Nilsson, I. Ragnarsson, P.J. Smith and E. Wallander, *J. Phys. G* **9**, 1217 (1983).
- 10) E.F. Moore, P.D. Cottle, C.J. Gross, D.M. Headly, U.J. Hüttmeier, S.L. Tabor and W. Nazarewicz, *Phys. Rev. C* **38**, 696 (1988).



- 11) E.F. Moore, P.D. Cottle, C.J. Gross, D.M. Headly, U.J. Hüttmeier, S.L. Tabor and W. Nazarewicz, *Phys. Lett.* B211, 14 (1988).
- 12) W. Fieber, K. Bharuth-Ram, J. Heese, F. Christancho, C.J. Gross, K.P. Lieb, S. Skoda and J. Eberth, *Z. Phys.* A332, 363 (1989).
- 13) U.J. Hüttmeier, C.J. Gross, D.M. Headly, E.F. Moore, S.L. Tabor, T.M. Cormier, P.M. Stwertka, and W. Nazarewicz, *Phys. Rev.* C37, 118 (1988).
- 14) S.L. Tabor, P.D. Cottle, C.J. Gross, U.J. Hüttmeier, E.F. Moore and W. Nazarewicz, *Phys. Rev.* C39, 1359 (1989).
- 15) G. Winter, J. Döring, L. Funke, H. Prade, H. Rotter, R. Schwengner, A. Johnson, and A. Nilsson, *J. Phys.* G14, L13 (1988).
- 16) L. Funke, F. Dönan, J. Döring, P. Kennitz, E. Will, G. Winter, L. Hildingsson, A. Johnson and Th. Lindblad, *Phys. Lett.* 120B, 301 (1983).
- 17) A.J. Kreiner and M.A.J. Mariscotti, *Phys. Rev. Lett.* 43, 1150 (1979).
- 18) Ikuko Hamamoto, *Phys. Lett.* B235, 221 (1990).